



1 **Climate change overtakes coastal engineering as the dominant driver** 2 **of hydrologic change in a large shallow lagoon**

3 Peisheng Huang^{1,2}, Karl Hennig³, Jatin Kala⁴, Julia Andrys⁴, Matthew R. Hipsey^{1,2}

4 ¹Aquatic Ecodynamics, UWA School of Agriculture and Environment, The University of Western Australia, Crawley WA
5 6009, Australia.

6 ²UWA Oceans Institute, The University of Western Australia, Crawley WA 6009, Australia.

7 ³Water Science Branch, Department of Water and Environmental Regulation, Perth WA 6842, Australia.

8 ⁴Environmental and Conservation Sciences, Murdoch University, Murdoch WA 6015, Australia.

9 *Correspondence to:* Peisheng Huang (peisheng.huang@uwa.edu.au)

10 **Abstract.** Ecosystems in shallow, micro-tidal lagoons are particularly sensitive to hydrologic changes. Lagoons are also highly
11 complex transitional ecosystems between land and sea, and the signals of direct human disturbance to the lagoon can be
12 confounded by variability of the climate system, but from an effective estuary management perspective the effects of climate
13 versus direct human engineering interventions need to be identified separately. Although many estuarine lagoons have
14 undergone substantial human interventions, such as artificial channels, the effects from the interaction of climate change with
15 engineering interventions have not been well evaluated. This study developed a 3D finite-volume hydrodynamic model to
16 assess changes in hydrodynamics of the Peel-Harvey Estuary, a large choked-type lagoon, considering how attributes such
17 as water retention time, salinity and stratification have responded to a range of factors, focusing on the drying climate trend
18 and the opening of a large artificial channel over the period from 1970 to 2016, and how they will evolve under current climate
19 projections. The results show that the drying climate has fundamentally changed the hydrology by comparable magnitudes to
20 that of the opening of the artificial channel, and also highlight the complexity of their interacting impacts. Firstly, the artificial
21 channel successfully improved the estuary flushing by reducing average water ages by 20-110 days; while in contrast the
22 reduced precipitation and catchment inflow had a gradual opposite effect on the water ages, and during the wet season this has
23 almost counteracted the reduction brought about by the channel. Secondly, the drying climate caused an increase in the salinity
24 of the lagoon by 10-30 PSU; whilst the artificial channel increased the salinity during the wet season, it has reduced the
25 likelihood of hypersalinity (>40 PSU) during the dry season in some areas. The impacts also varied spatially in this large
26 lagoon. The southern estuary, which has the least connection with ocean through the natural channel, is the most sensitive to
27 climate change and the opening of the artificial channel. The projected future drying climate is shown to slightly increase the
28 retention time and salinity in the lagoon, and increase the hypersalinity risk in the rivers. The significance of these changes for
29 nutrient retention and estuary ecology are discussed, highlighting the importance of these factors when setting up monitoring
30 programs, environmental flow strategies and nutrient load reduction targets.

31 **1 Introduction**

32 Hydrologic features such as water circulation and retention, and the pattern of saline water intrusion, are critical in shaping
33 estuarine ecosystems. The interactions between freshwater runoff pulses with ocean water can create complex hydrodynamics
34 that subsequently structures coastal biogeochemical processes, including the distribution of sediment and nutrients, and areas
35 favourable for primary productivity (e.g. Cloern et al., 2017; Kasai et al., 2010; Legović et al., 1994; Watanabe et al., 2014).
36 Whilst nutrient loads are the primary determinant affecting the long-term trophic state of coastal waters (Howarth and Marino,
37 2006; Williamson et al., 2017), the time-scales associated with water retention and mixing are critical in mediating the
38 relationship between nutrient inputs and the ensuing water quality response, including the likelihood of nuisance algal blooms
39 or hypoxia (e.g. Ferreira et al., 2005; Knoppers et al., 1991; Paerl et al., 2006; Zhu et al., 2017). The retention of water and



40 hydrodynamic patterns that emerge in any given site are largely dependent upon local geomorphological features, though
41 increasingly coastal engineering and changes in river hydrology disturb natural patterns of water exchange (Almroth-Rosell et
42 al., 2016; Dufour et al., 2001; Gong et al., 2008; Kjerfve et al., 1996; Knoppers et al., 1991; Odebrecht et al., 2015) .
43 Understanding and predicting these hydrologic changes is critical to underpin adaptive approaches to estuary water quality
44 management and ecological restoration.

45
46 Coastal lagoons and embayments with low rates of ocean exchange are particularly sensitive relative to other estuary forms.
47 The typical low flushing rates leads to high rates of deposition of sediment and particulate matter, and accumulation of nutrients
48 (e.g. Newton et al., 2014, 2018; Paerl et al., 2014). They are also productive ecosystems and often experience conflicting
49 interests between the ecosystem services they provide and the pressures from urban development and agricultural expansion
50 (Basset et al., 2013; Newton et al., 2014; Pérez-Ruzafa et al., 2011; Petersen et al., 2008; Zaldívar et al., 2008). In most cases,
51 salt intrusion mediates lagoon salinity and drives a difference between the surface and bottom salinity (salinity stratification).
52 In highly seasonal systems this effect leads to notable oxygen depletion and establishes hypoxia in the bottom boundary layer
53 (Bruce et al., 2014; Cottingham et al., 2014; Huang et al., 2018). In Mediterranean climate regions, further concerns of
54 hypersalinity through evaporation during the long dry summer and autumn months also exist (Potter et al., 2010). As a result,
55 the hydrodynamics of coastal lagoons are frequently modified through the creation of artificial channels built to enhance
56 hydrologic connectivity to the ocean, and increase nutrient export (e.g. Breardley 2005; Manda et al., 2014; Prestrelo and
57 Monteiro-Neto, 2016), or indirectly by engineering projects associated with dredging and coastal management (e.g. Ghezzeo et
58 al., 2010; Sahu et al., 2014).

59
60 Changes in lagoon hydrology result from variability in river flows, and meteorological and ocean conditions, alongside
61 (sporadic) human interventions associated with coastal engineering developments. Tracking these long-term changes remains
62 an ongoing challenge since the signals of human disturbance are often confounded by variability of the climate system and
63 lost in the dynamic estuarine conditions (Cloern et al., 2016; Feyrer et al., 2015). Although the impacts of climate change on
64 estuarine hydrology have been shown to significantly affect the water quantity and quality of many estuaries (e.g. Ducharme
65 et al., 2007; Liu and Chan, 2016; Lloret et al., 2008; Whitehead et al., 2009), the interacting effects of introducing human
66 interventions in conjunction with climate change trends are not necessarily easy to predict. For example, the opening of an
67 artificial channel and a drying climate can both introduce more ocean water into an estuary. On the other hand, the drying
68 climate enhances water residence time, which may cancel out flushing benefits from the artificial channel. The combined
69 effects are further complicated in large lagoon-type estuaries with complex morphology, where complicated patterns of water
70 retention and stratification can develop (e.g. Ferrarin et al., 2013). From a lagoon management perspective, it is necessary to
71 attribute the impacts from climate and human activity factors to better plan the necessary estuary and catchment management
72 activities, including adaptation strategies for associated with nutrient load targets and, in some cases, environmental water
73 provision.

74
75 Here we explore these ideas through reconstruction of the long-term hydrologic evolution of a large estuarine lagoon in
76 Western Australia: the Peel-Harvey Estuary (PHE). The PHE system has been subject to both a notable drying climate trend
77 and substantial coastal modification in the form of an opening of a large artificial channel, coastal development and dredging.
78 The artificial channel, termed the “Dawesville Cut” (hereafter referred as “the Cut”), was built in 1994 with the purpose of
79 increasing the flushing of the lagoons and reducing nutrient concentrations. In parallel, the impact on inland water resources
80 of recent climate trends has been particularly acute in the PHE catchment, which was acknowledged by the IPCC AR4
81 identifying this region as one that has experienced amongst the greatest impact on divertible water resources in the world



82 (Bates et al., 2008; Izrael et al., 2007). From the 1970s, rainfall has decreased by 16% and stream flows have declined by more
83 than 50%, a trend which has appeared to accelerate since the 2000s (Silberstein et al., 2012). Whilst the nutrient and
84 phytoplankton concentrations have been successfully reduced by the construction of the channel (Brearley, 2005), the long-
85 term river flows have shown a clear trend of decreasing inputs to the estuary with concerns for the conditions of the tidal
86 riverine portions of the system (Gillanders et al., 2011; Hallett et al., 2018). A series of water quality improvement plans (e.g.
87 Environmental Protection Authority, 2008; Rogers et al., 2010) continue to be developed to promote estuary health, however,
88 ongoing concerns about the current and future water quality and ecologic condition of the system (Valesini et al., 2019) requires
89 knowledge of spatiotemporal changes in water retention, stratification and salinisation to support adaptation efforts.

90

91 It is therefore the aim of this study to develop a methodology to disentangle drivers of change of the PHE system, over the
92 period from 1970 to 2016, and outline the expected future trajectory of lagoon conditions. To this end we employ a 3-
93 dimensional finite-volume hydrodynamic model for analysis of environmental drivers on estuarine hydrology by comparing
94 current and counter-factual modelling scenarios to enable attribution of the drivers of change. To enable the long-term
95 reconstruction of the model simulations for periods before the instrument record, and for future conditions, we drive the model
96 with a hybrid set of weather and hydrological boundary condition data from observations and supporting models. The results
97 of simulations are presented to analyse the sensitivity of water retention time, salinity and stratification within the lagoon to
98 selected factors. By untangling the effect of the drying climate versus the Cut opening, through time and space, we explore the
99 results through the lens of nutrient load reduction targets and biodiversity management implications. We anticipate the
100 approach adopted here can be useful to assist in the climate change adaptation efforts for other estuarine lagoons in mid-
101 latitude regions.

102

103 **2 Methods**

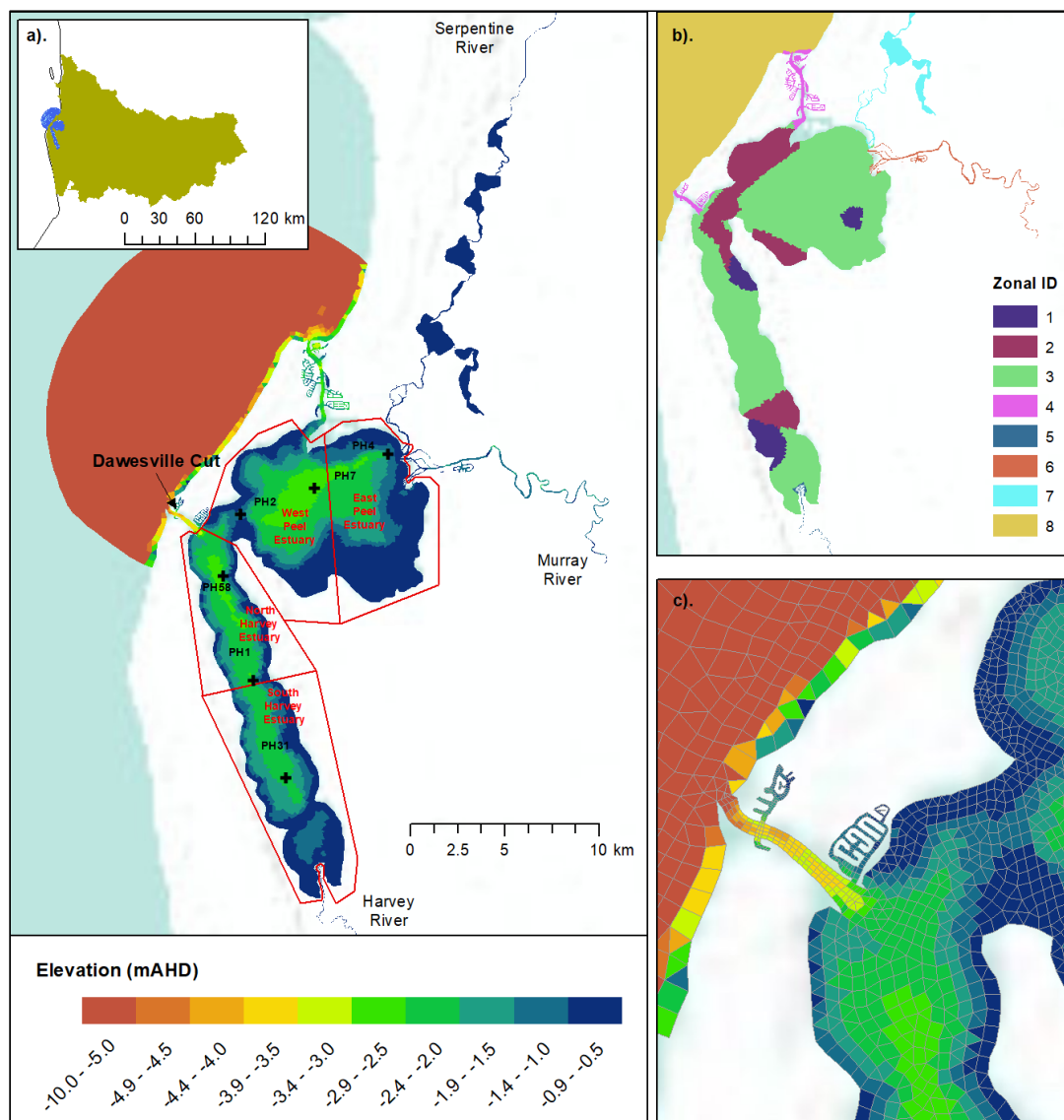
104 **2.1 Site description**

105 PHE is a large shallow coastal estuary-lagoon system located approximately 75 km south of Perth in Western Australia (Figure
106 1), which is listed under the Ramsar convention for wetlands of international significance. The estuary has a complex
107 morphometry and comprises two shallow lagoons, one is the Peel Inlet, a circular inlet to the north, and the other the Harvey
108 estuary, an oblong lagoon attached to the Peel Inlet at its north-eastern edge, with a combined area of approximately 133 km².
109 The estuary experiences a micro-tidal regime (tidal range < 1 m) and connects to the ocean via two channels: 1) the Mandurah
110 Channel, a natural but narrow 5 km long channel with water depths varying between 2 m and 5 m; and 2) the Cut, an artificial
111 channel of about 2.5 km long, 200 m wide and between 6 and 6.5 m deep, built in 1994 (Bicknell, 2006; Environmental
112 Protection Authority, 2008). The coastal catchment of the estuary is drained by three major river systems: the Serpentine,
113 Murray and Harvey Rivers (Figure 1), and numerous minor drains. The riverine portions depicted are tidal and experience
114 marine water intrusion for extended periods throughout the year. The system experiences a Mediterranean-type climate
115 characterised by a strong seasonal pattern of cool wet winters and hot dry summers, with almost all of the annual rainfall
116 occurring during the cooler months of May to October (Finlayson and McMahon, 1988; Gentili, 1971).

117

118

119



120

121 **Figure 1.** (a) Model domain of the Peel-Harvey Estuary and three main rivers: Serpentine River, Murray River, and Harvey
122 River, the tidal portion of each is depicted up to the gauge location. The colours indicate the water depths of the study domain;
123 the black crosses within the estuary indicate the 6 monitoring sites, and the red polygons indicate the areas for result analysis.
124 (b) Zonal categorization of the model domain according to the area and aquatic vegetation biomass (see Table 1), and (c) a
125 zoom-in view of the artificial channel Davesville Cut, constructed in 1994 to improve ocean flushing.

126

127

128 2.2 Modelling Approach

129 2.2.1 Hydrodynamic model and numerical methods

130 The TUFLOW-FV (BMT WBM, 2013) hydrodynamic model was adopted, using a flexible-mesh (finite volume) approach to
131 resolve the variations in water level, horizontal salinity distribution and vertical density stratification in response to tides,



132 inflows and surface thermodynamics. The mesh consists of triangular and quadrilateral elements of different size that are suited
 133 to simulating areas of complex estuarine morphometry. To meet accuracy requirements, fine-grid resolution (mean mesh area
 134 $\sim 12000 \text{ m}^2$) was used within the lagoons and coarse resolution was implemented towards the ocean boundary. The vertical
 135 mesh discretization adopted a hybrid sigma-z coordinate allowing multiple surface Lagrangian layers to respond to tidal
 136 elevation changes. The layer thickness was 0.2 m at depths of 1.0 – 5.0 m that gradually increased to 0.5 m in deeper water
 137 and then five uniformly-distributed sigma layers were then added above the fixed-thickness layers. The finite volume
 138 numerical scheme solves the conservative integral form of the nonlinear shallow water equations in addition to the advection
 139 and transport of scalar constituents such as salinity and temperature. The equations are solved in 3D with baroclinic coupling
 140 from both salinity and temperature using the UNESCO equation of state (Fofonoff and Millard, 1983).

141
 142 Surface momentum exchange and heat dynamics are solved internally within TUFLOW-FV. In the current application,
 143 turbulent mixing of momentum and scalars has been calculated using the Smagorinsky scheme in the horizontal plane and
 144 through coupling with the General Ocean Turbulence Model (GOTM) for vertical mixing with option of second-order k- ϵ
 145 turbulence closure. The bottom shear stress was calculated using a roughness-length relationship assuming a rough-turbulent
 146 logarithmic velocity profile in the lowest model layer. The roughness length, z_0 , settings were based on the area type (e.g.
 147 coast, rivers, and estuary) and the estimated biomass of aquatic vegetation within the cell. For this purpose, the modelling
 148 bottom was categorized into eight zones (Figure 1b) where the benthic characteristics and associated z_0 in each zone were
 149 specified (Table 1). While the setting of z_0 affected the water advection and uncertainty remains in the spatial (and temporal)
 150 variability in the z_0 , it is important to note that the modelled τ and salinity do not change fundamentally over a reasonable
 151 range of z_0 , as shown in the results of the model sensitivity tests described later.

152

153 **Table 1.** Zonal characters and roughness length z_0 setting in the model domain.

Zonal ID	Areas	Aquatic Vegetation Biomass (g Dry Weight/m ²)	z_0
1	South/North Harvey Estuary, East Peel Inlet	100-230	0.03
2	South/North Harvey Estuary, West Peel Inlet	50-100	0.02
3	Harvey Estuary and Peel Inlet	0-50	0.01
4	Dawesville Cut	N/A	0.003
5	Harvey River	N/A	0.003
6	Murray River	N/A	0.003
7	Serpentine River	N/A	0.003
8	Coastal ocean	N/A	0.002

154

155 The water retention time was assessed with two hydrodynamic time parameters. The first was water age, which was defined
 156 as the time the water had spent since entering the estuary through boundaries (either the ocean or rivers). The water age, τ ,
 157 was computed in each computational cell using the AED2 plugin to the hydrodynamic model, which simulated a conservative
 158 tracer subject to a constant increase with time (‘aging’) and mixing, using a method as described in (Li et al. 2019). This
 159 method therefore provided the temporal and spatial variation in water retention, $\tau = \tau(x, y, z, t)$. The second time parameter
 160 was the bulk flushing time, τ_f , which represents a bulk retention parameter that assumes a fully-mixed ‘lumped’ approach and
 161 describes the general exchange character of the estuary (Monsen et al., 2002). Following Sheldon and Alber (2006), the bulk
 162 flushing time was calculated as:

163
$$\tau_f = \frac{V}{Q_{FW} + R_o Q_{SW}}$$



164 where V is the estuary volume (=187.5 GL), Q_{FW} is the freshwater inflow rate, Q_{SW} is the average seawater flow rate over a
165 tidal period, and R_o is the exchange fraction of the seawater fluxes that contributes to flushing. The values of Q_{FW} and Q_{SW}
166 are derived from the hydrodynamic model outputs. The value of R_o is dependent upon the local coastal mixing features
167 (Fischer et al., 1979; Rynne et al., 2016; Shi et al., 2019), and was set to 0.15 for Mandurah Channel and 0.12 for the Cut.

168

169 Multiple concepts of hydrodynamic time parameters (flushing time, residence time, water age, export time, etc.) have been
170 used in coastal hydrology research and their comparison has been intensively discussed (e.g. Jouon et al., 2006; Mosen et al.,
171 2002; Sheldon and Alber, 2006), noting that each of the parameters are different in their definition and application. Here, we
172 used the time parameters to investigate how the bulk flushing time and the heterogeneity of the local water age changed in
173 response to the climate induced changes and the opening of the Dawesville Cut.

174

175 **2.2.2 Climate change context and simulation rationale**

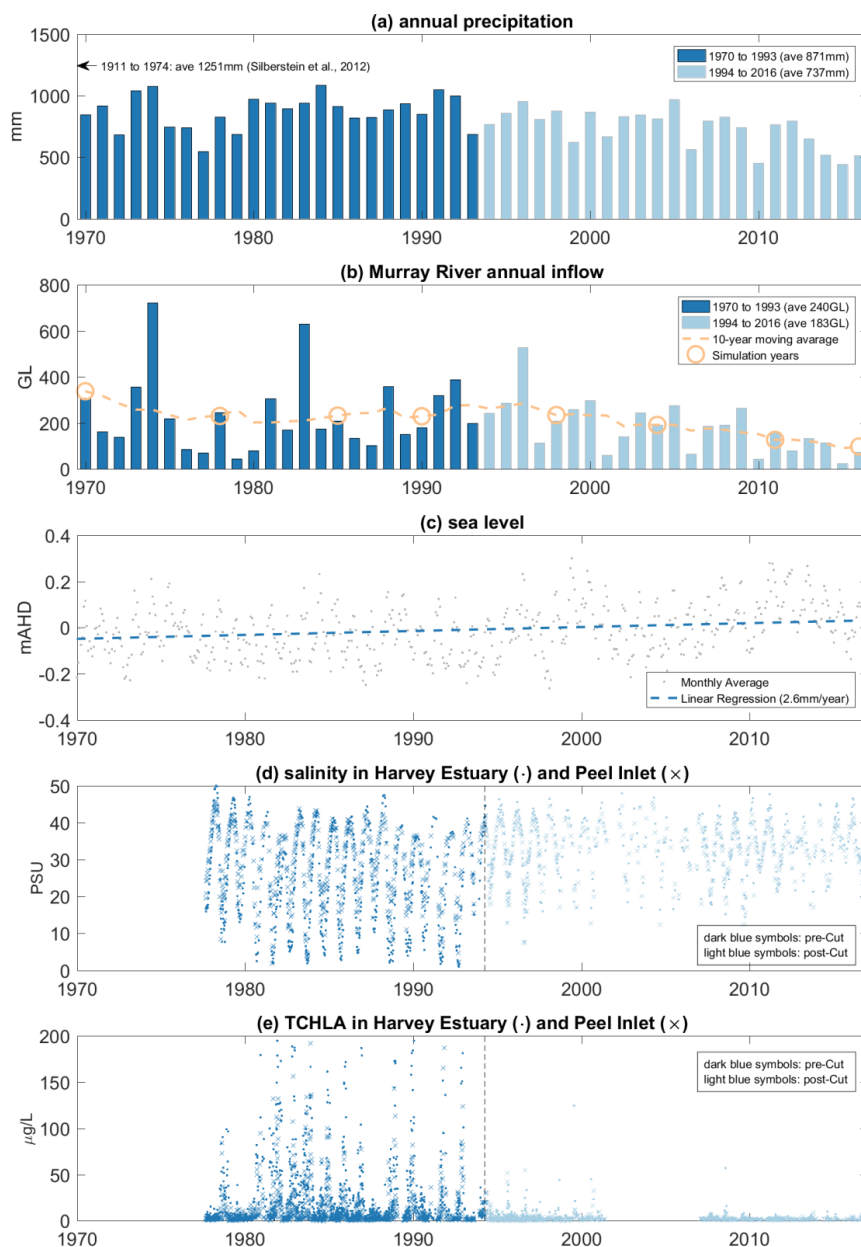
176 Historical observations of nearby precipitation and the gauged data of the major Murray River inflow have shown a decreasing
177 trend from 1970 to the present (Figure 2), though variability from year to year is noticeable. The average annual precipitation
178 has declined by 15% when comparing the period 1994-2016 relative to 1970-1993, and this led to a dramatic decrease of
179 annual inflow volumes, most notable in the past decade.

180

181 Years with inflow rates close to the 10-year moving average were selected for hydrologic modelling simulations to explore in
182 more detail the hydrologic changes occurring within these years (depicted relative to the trend in Figure 2b). Due to the concern
183 that the drying climate will continue into the 21st century (Silberstein et al., 2012; Smith and Power, 2014), we also undertook
184 model simulations to investigate potential hydrologic changes under future conditions representative of 2040 and 2060, by
185 considering reduced streamflow and rising sea levels. The runoff declines were based on the mean projection by Smith and
186 Power (2014) that suggested the total runoff to the rivers and estuaries within the WA region will drop by about 0.96% per
187 year, corresponding to the projected reduction in precipitation of 0.27% per year, on average. Sea level rise was also included
188 in the future scenarios, estimated from the long-term (1897 – 2000) tide gauge observations at the Fremantle tide gauge station
189 that shows a sea level trend of 1.50 mm/yr (Kuhn et al., 2011). These estimates may be biased due to a possible accelerated
190 sea level rise towards the end of the 21st century (IPCC, 2007; Kuhn et al., 2011), but we highlight these future scenarios were
191 set up with a focus to investigate the changing hydrology into a future from the projected drying climate trend.

192

193 For the modelling years after 1994, when the artificial channel was constructed, we also ran “no-Cut” counter-factual scenarios,
194 which assumed the Dawesville Cut engineering intervention was not constructed, in order to separate the impact of the artificial
195 channel on hydrology relative to the “with-Cut” scenarios (Table 2).



196

197 **Figure 2.** Historical record of (a) annual precipitation rate; (b) Murray River annual inflow rate; (c) monthly-average sea level
198 at Fremantle gauge station; (d) salinity at Harvey Estuary and Peel Inlet; and (e) total chlorophyll-a (TCHLA) in Harvey
199 Estuary and Peel Inlet since 1970 to 2016.

200

201

202 Gauged flow rate data for the Murray River, Serpentine River and Harvey River were applied to the hydrodynamic model
203 whenever they are available. For the missing periods in the gauged flows and the ungauged drains, the output from the Source



204 (eWater®) catchment modelling platform (Kelsey et al., 2011; Welsh et al., 2013), operated by the Western Australia
 205 Department of Water and Environmental Regulation, was used to estimate flows by carefully comparing the measured and
 206 modelled flow data. Groundwater inputs was previously estimated to represent only ~1% of total water inputs (Black and
 207 Rosher, 1980), and therefore was ignored from the modelling simulations.

208

209 Various data sources were used to set up meteorological inputs due to the study period spanning a long time back to 1970,
 210 when meteorological observations were not routinely available across the modelling domain at hourly frequencies. The first
 211 data source was the local Mandurah weather station located beside the natural channel of the estuary. This dataset provided
 212 hourly records since 2001. The hourly fields over the period 1981–2000 were obtained from regional climate model simulations
 213 for Southwest Australia at a 5 km resolution (Andrys et al., 2015; Kala et al., 2015). These simulations were carried out using
 214 the Weather Research and Forecasting (WRF), one of the most widely used regional climate models. Andrys et al. (2015)
 215 showed that the WRF model was able to adequately simulate the climate of SWA, and these simulations have also been used
 216 to assess the impacts of current and future climate on temperature and precipitation (Andrys et al., 2016, 2017) as well as
 217 climate indices relevant to viticulture for SWA (Firth et al., 2017). The WRF simulations of Andrys et al. (2015) have also
 218 been benchmarked against other regional climate model simulations across the Australian continent and shown to perform
 219 well in simulating both temperature and precipitation (Di Virgilio et al., 2019) as well as heat-wave events (Hirsch et al.,
 220 2019). For the years before 1981 the weather conditions measured at the nearby Halls Head weather station (4.2 km away
 221 from the Mandurah station) were used.

222

223 A summary of all historical simulations and future scenarios is provided in Table 2. The total inflow into the estuary of the
 224 chosen simulation years shows a general decrease from past to future, except for the year 1978 when the total inflow rate was
 225 less than that in 1985 and 1990. This was due to an exceptionally low inflow rate within the Harvey River, produced from the
 226 catchment model output, which had an effect mostly on the Harvey Estuary. We still include this year to show the historical
 227 evolution during the past decades.

228

229

230 **Table 2.** Summary of simulated scenarios and their annual precipitation, catchment inflow volumes, mean sea level, and Cut-
 231 opening information.

Simulation Category	Simulated Year	Annual precipitation (mm)	Annual Catchment Inflow (GL)	Annual Mean Sea Level (mAHD)	Cut Opening	Sensitivity tests
<i>Pre-Cut years</i>	1970	846.4	705.9	-0.043	No	
	1978	827.5	591.6	-0.024	No	
	1985	911.7	564.0	-0.033	No	
	1990	849.2	515.8	-0.071	No	Yes
<i>Post-Cut years</i>	1998	876.2	490.4	-0.027	Yes	Yes
	2004	813.7	478.0	-0.027	Yes	
	2011	766.0	378.9	0.156	Yes	
	2016	514.4	244.2	0.017	Yes	
<i>No-Cut scenarios</i>	1998	876.2	490.4	-0.027	No	
	2004	813.7	478.0	-0.027	No	
	2011	766.0	378.9	0.156	No	
	2016	514.4	244.2	0.017	No	
<i>Future Scenarios</i>	2040	481.1	187.9	0.053	Yes	
	2060	453.3	138.9	0.083	Yes	
	2040	481.1	187.9	0.053	No	
	2060	453.3	138.9	0.083	No	

232



233

234 **2.2.3 Model performance evaluation and sensitivity tests**

235 The model accuracy in reproducing the key hydrologic features was assessed by using the salinity and temperature data
236 measured at six monitoring stations along the estuary (Figure 1). Monthly salinity and temperature datasets were obtained
237 from the Marine and Freshwater Research Laboratory of the Murdoch University (1977-2001) and the Western Australia
238 Water Information Reporting website (<http://wir.water.wa.gov.au/>) (2002-2017). For each variable, we evaluated the model
239 quantitatively against the monitored data using three skill metrics: correlation coefficient (r), mean absolute error (MAE), and
240 model skill score (SS). Comprehensive evaluation was conducted for all the simulation years, except for 1970 when the long
241 term monitoring had not started yet. The evaluation focused on the salinity and water temperature of the surface and bottom
242 water at the 6 monitoring stations within the estuary. Surface elevation records obtained from the gauged stations in the centre
243 of Peel Inlet, provided by the Department of Transport of Western Australia, were also used to validate the modelled surface
244 elevation in year 1990 (a modelled year before the Cut opening) and 1998 (a modelled year after the Cut opening).

245

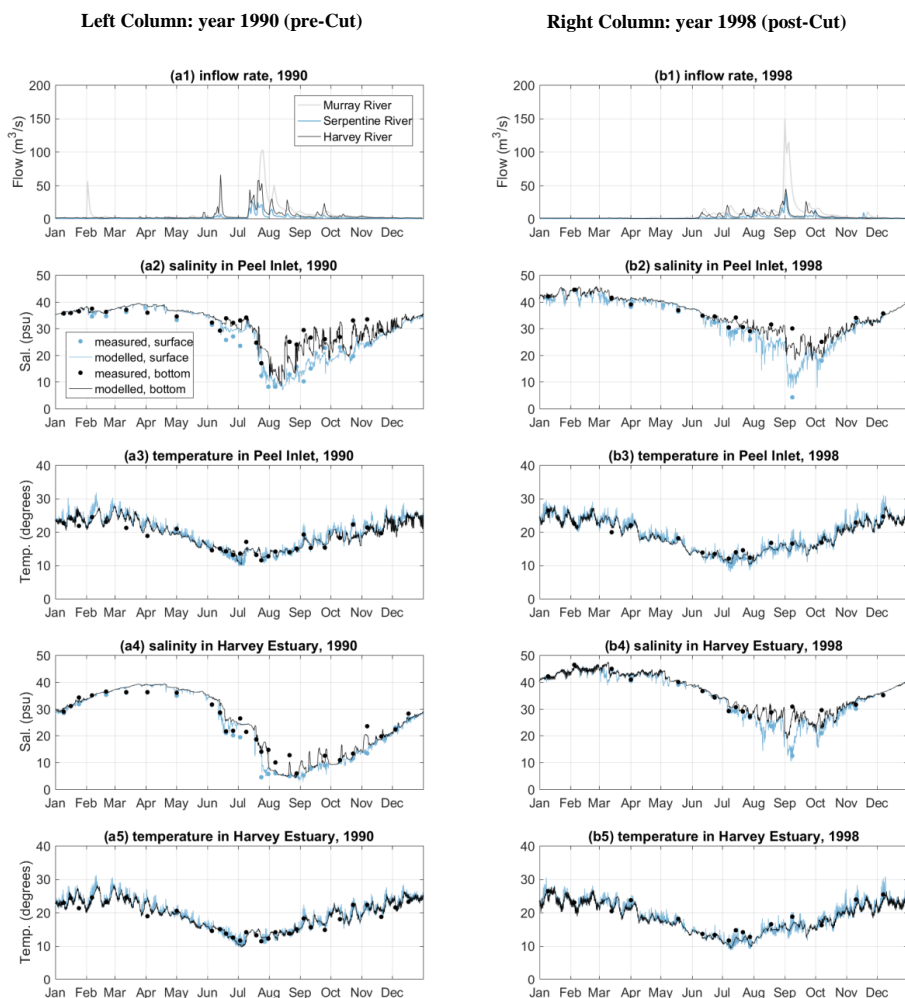
246 The current study focused on the impact of reduced inflow, due to drying climate and the Cut, on the estuary hydrology.
247 However, the perturbations of environmental factors such as air temperature, tide elevation, and benthic vegetation could also
248 affect the local hydrology, and so their influence on the modelling results was explored. To evaluate the effects of these factors,
249 the sensitivity of the τ and salinity was assessed relative to changes in: (1) air temperature (± 1 degree, representing 100 year
250 change of local air temperature); (2) tidal elevation (± 0.15 m, representing 100 year change of local tide record); and (3) bed
251 roughness length ($\pm 50\%$, representing 50% change of bed roughness). The ranges of these environmental factors were carefully
252 selected based on the historical records. Two years, 1990 and 1998, representing a year before the Cut-opening and another
253 year with the Cut, respectively, were selected for these model sensitivity tests.

254 **3 Results**

255 **3.1 Model reconstruction of historical conditions**

256 The monitored and modelled salinity and temperature at the centres of the two lagoons in the pre- and post-Cut years
257 demonstrate the ability of the model to accurately capture the seasonal cycle in response to the catchment inflows (Figure 3).
258 In summer and early autumn the flow rates were low, followed by high salinity and weak salinity stratification in the two
259 lagoons. In contrast, there were large inflows to the estuary in winter and early spring. The peaks of the inflows occurred in
260 winter (July – September), followed by a significant drop in the salinity in the estuary due to the freshwater flushing. However,
261 differences in the salinity response to freshwater flushing can be observed between the pre-Cut year (1990, left column of
262 Figure 3) and the post-Cut year (1998, right column of Figure 3). In 1990 when the estuary had limited connection without the
263 opening of the Cut, the salinity stratification was small in the Harvey Estuary. The salinity dropped to below 5 PSU, indicating
264 the hydrology of Harvey Estuary was mainly dominated by the Harvey River flushing. Whilst during 1998, with greater ocean
265 connection due to the opening of the Cut, stronger salinity stratification was observed in the Harvey estuary, and the minimum
266 salinity was lifted to over 10 PSU due to more seawater intrusion from the Cut. The water temperature also showed a clear
267 seasonal signal, ranging from about 10 °C in winters to 30 °C in summers. The differences in the water temperature observed
268 in the centres of two lagoons, and between the surface and bottom waters, were small.

269



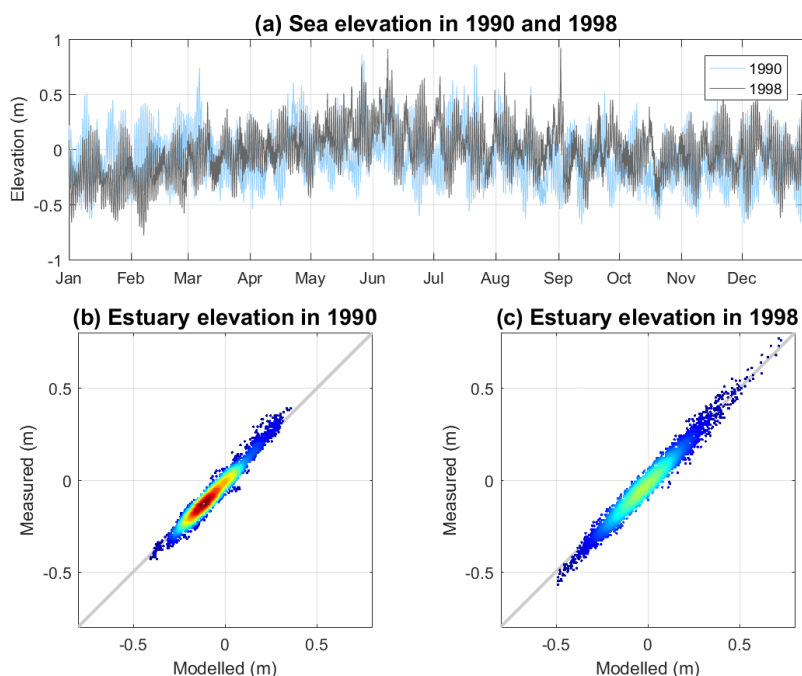
270

271 **Figure 3.** Annual variation in 1990 (left column, a) and 1998 (right column, b) of (1) inflow rate of the three main rivers; (2)
272 monitored and modelled surface and bottom salinity at the centre of Peel Inlet (site PH7 at Figure 1); (3) monitored and
273 and modelled surface and bottom water temperature at the centre of Peel Inlet; (4) monitored and modelled surface and bottom
274 salinity at the centre of Harvey Estuary (site PH1 at Figure 1); (5) monitored and modelled surface and bottom water
275 temperature at the centre of Harvey Estuary;

276

277 The opening of the Cut also affected the surface elevations of the estuary (Figure 4). The tide elevations in the ocean showed
278 similar characteristics in 1990 and 1998 in terms of the annual mean sea level (-0.071 mAHD and -0.027 mAHD in 1990 and
279 1998, respectively) and tidal range (both < 1 m). However, the surface elevation measured at the centre of the estuary had
280 significantly different characteristics in these two years. The estuary surface elevation in 1998 had a much wider range of -0.6
281 m to 0.8 m compared to that in 1990 of -0.4 m to 0.4 m, indicating an enlarged tidal-prism and higher magnitude of water
282 exchange with the ocean due to the opening of the Cut.

283



284

285 **Figure 4.** (a) Sea level variation in 1990 and 1998; (b) modelled vs. measured surface elevation in the centre of Peel Inlet in
 286 1990 ($r=0.9795$), the grey line indicates the 1:1 ratio; and (c) same as figure b except for year 1998 ($r=0.9841$). The colour
 287 from blue to red in figure b and c indicates the data density from minimum to maximum.

288 In general, the model reproduced the temporal variations of salinity and temperature in both the surface and bottom well (Table
 289 3). The mean regression coefficient r for the salinity from six monitoring sites is above 0.81, and for the water temperature is
 290 above 0.85 except in the year 1970, when a mean r of 0.72 was obtained, which may have been due to poor boundary forcing
 291 for this year. The model skill scores are generally higher than 0.61 for both salinity and temperature in all historical years,
 292 suggesting the model has captured the major features of the hydrodynamic response to the external forcing of tide and
 293 freshwater inputs.

294

295 **Table 3.** Summary model performance statistics at 6 monitoring stations (indicated as dark crosses in Figure 1) in the selected
 296 historical years.

297

298

Simulated year	Model performance of salinity (mean±std)			Model performance of temperature (mean±std)		
	r	MAE	SS	r	MAE	SS
1970	N/A	N/A	N/A	N/A	N/A	N/A
1978	0.95±0.02	3.24±0.54	0.85±0.02	0.72±0.16	1.89±1.10	0.58±0.23
1985	0.97±0.01	2.18±0.14	0.92±0.01	0.97±0.01	0.94±0.09	0.91±0.03
1990	0.95±0.02	2.60±0.18	0.87±0.05	0.94±0.02	1.31±0.10	0.81±0.04
1998	0.94±0.03	2.04±0.43	0.74±0.29	0.95±0.02	1.66±0.28	0.73±0.14
2004	0.81±0.20	3.78±1.47	0.61±0.34	0.85±0.05	1.60±0.28	0.62±0.15
2011	0.88±0.14	3.69±0.84	0.75±0.19	0.94±0.03	1.43±0.19	0.65±0.15
2016	0.87±0.11	3.54±0.81	0.74±0.23	0.96±0.01	1.13±0.08	0.88±0.02



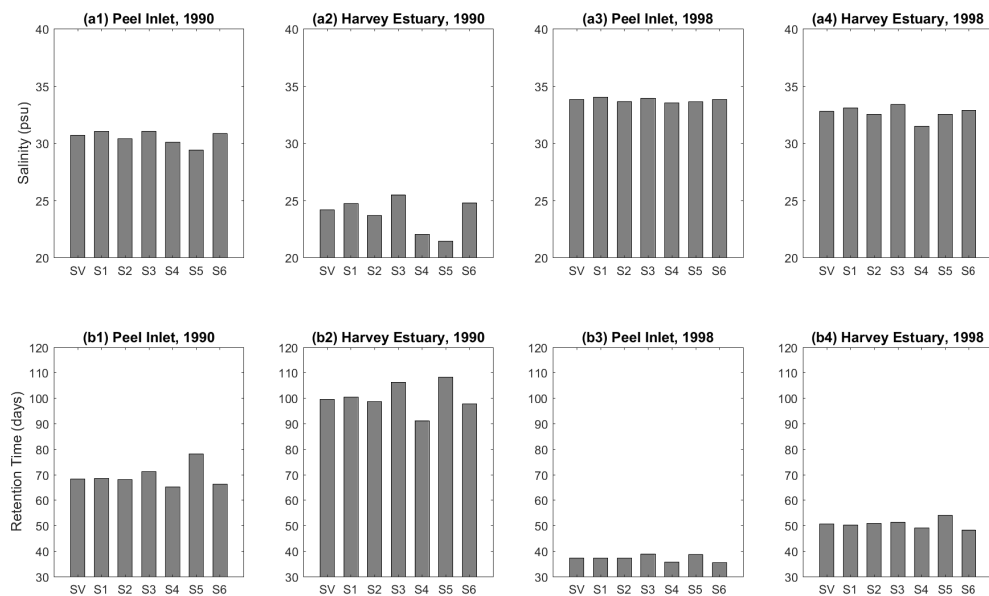
299

300 3.2 Sensitivity to air temperature, benthic properties, and sea level variation

301 The sensitivities of modelled salinity and τ to air temperature, tide elevation, and bed roughness are shown in Figure 5. The
302 changes in the air temperature of ± 1 °C have minor effects on both the salinity and τ in both years of 1990 and 1998. The
303 influence of air temperature on the hydrology was mostly through evaporation, and resulted in changes in salinity of less than
304 0.9 PSU, and 0.5 days changes in τ . Secondly, the changes in the mean tide elevation of ± 0.15 m led to changes in salinity of
305 up to 2.2 PSU and 8.4 days in τ . Thirdly, the bed friction also had a noteworthy impact on the salinity and τ by modifying the
306 water movement and therefore benthic layer mixing at near-bed level. The presence of benthic vegetation was shown to affect
307 salinity by up to 2.8 PSU in the Harvey Estuary, while a maximum change in the τ of 8.6 days was observed in the same
308 location.

309 In summary, the modelled salinity and τ were affected by the changes in the sea level variation and bottom vegetation presence,
310 but the effects of these environmental factors were still small when compared to that caused by the reduced flow over the past
311 decade and the Cut-opening, which is shown in the next sections. For example, the maximum change in τ observed in the
312 sensitivity test runs was 8.6 days, caused by the enhanced bottom roughness in the 1990 scenario, compared to the magnitude
313 of 20-100 days caused by the reduced flow from 1970 to 2016 (see more details in below). The maximum changes in the
314 salinity observed in the sensitivity test runs was 2.8 PSU, caused by the reduction of tide level in the Harvey Estuary, compared
315 to the magnitude of 10-30 PSU changes in the salinity caused by the reduced flows from 1970 to 2016 (see more details in
316 below).

317



3

319 **Figure 5.** Sensitivity of the modelled annual-mean salinity and retention time in the Peel Inlet and Harvey Estuary. SV:
320 standard scenario; S1: +1 degree in air temperature scenario; S2: -1 degree in air temperature scenario; S3: +0.15 m in tide
321 elevations scenario; S4: -0.15 m in tide elevations scenario; S5: +50% in bed roughness scenario; S6: -50% in bed roughness
322 scenario.

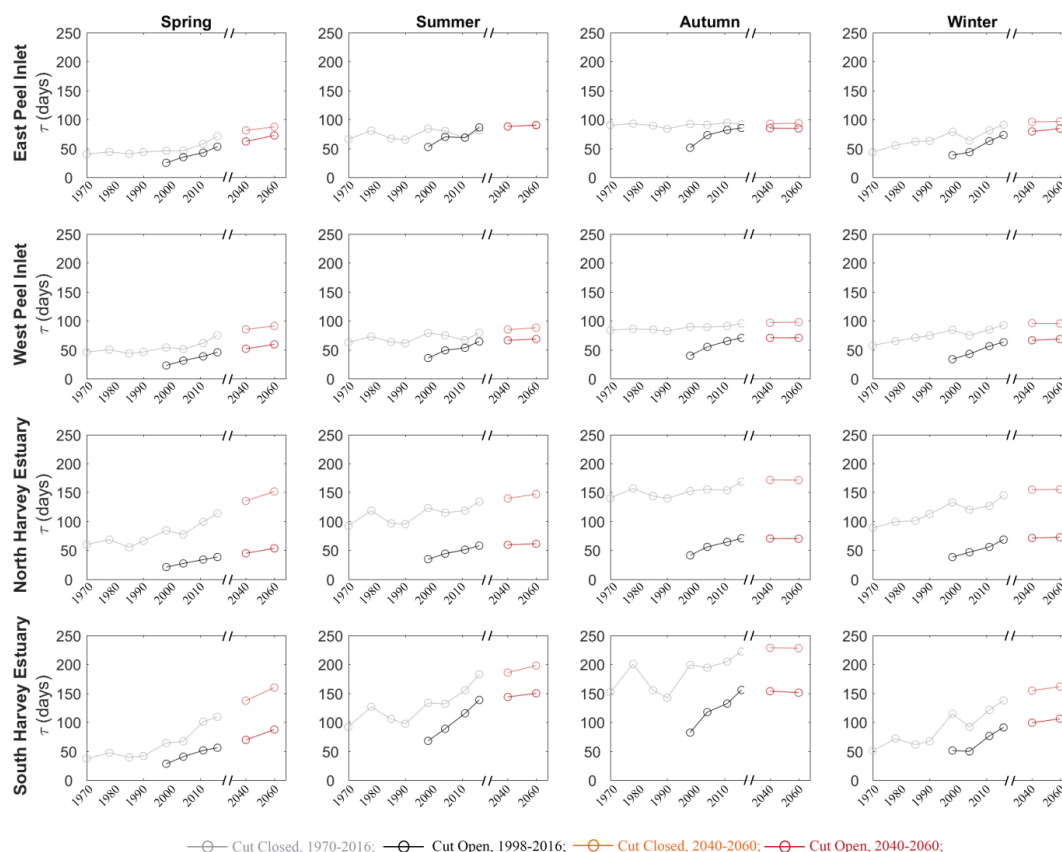


323

324 **3.3 Response of water retention to climate change and Cut-opening**

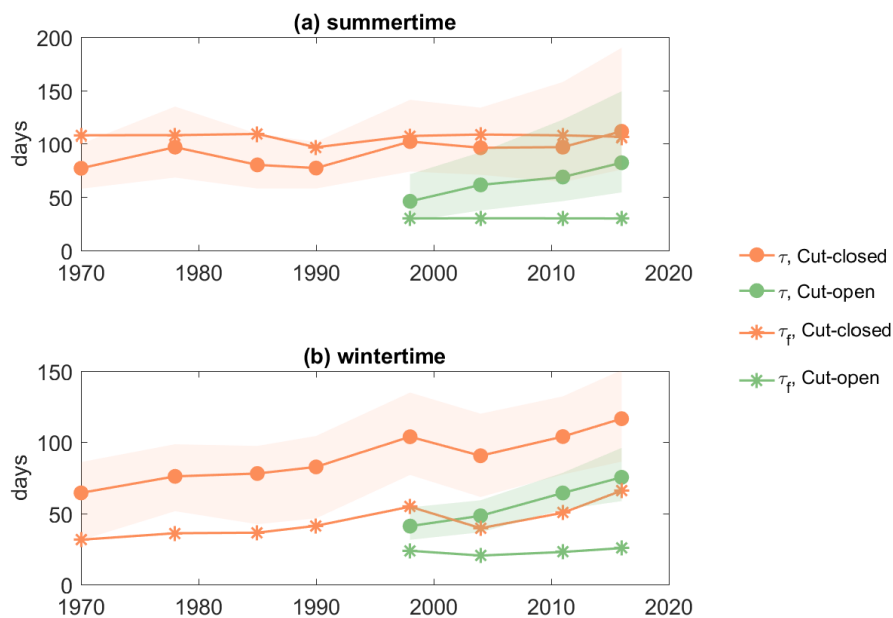
325 Water retention is highly dynamic depending on seasonal flows, tidal conditions, and in different regions of the estuary. The
326 evolution of water age, τ , over time has shown a general increase from 1970 to the present, superimposed on the effect of the
327 Cut, however, with some considerable variation across the two lagoons (Figure 6). Firstly, the wet season (winter and spring)
328 was more sensitive to the changes in the drying climate. In the “no-Cut” scenarios (assuming the artificial channel was not
329 constructed), it was predicted that τ would have increased in the Peel Inlet from about 50 days in 1970 to nearly double in
330 2016, and increased from approximately 50 days in 1970 to nearly 150 days in 2016 in the Harvey Estuary, solely due to the
331 drying climate trend. In contrast, the dry season (summer and autumn) conditions did not show significant changes over time
332 in most parts of the estuary, except in the south Harvey Estuary, which is furthest from the channels. The opening of the Cut
333 had a prominent effect by reducing τ by about 20-45 days in the Peel Inlet, and more profoundly by 50-100 days in the Harvey
334 Estuary. Yet the drying climate effect on the water age has largely cancelled out the flushing effect by the Cut in some regions.
335 The increases in τ from 1998 to 2016, due to reduced inflows, are of the same magnitude as the level of reduction caused by
336 the Cut opening. For example, the Cut opening reduced the τ by 28 days in the west Peel Inlet in 1998, yet the τ increased by
337 27 days from 1998 to 2016 due to the reduced flows. Lastly, the Harvey Estuary was most influenced by the climate changes
338 and the Cut opening. North Harvey Estuary, directly adjacent to the Cut, was most impacted by the Cut opening, and the τ was
339 reduced by more than 110 days. The south Harvey Estuary, which is furthest from both the channels, was more sensitive to
340 climate change, showing the greatest variation over the most recent decade. The projected climate is expected to increase the
341 τ further in the Harvey Estuary in spring, but a relatively smaller impact at other sites and seasons.

342



344 **Figure 6.** Mean water retention time, τ , in east Peel Inlet, west Peel Inlet, north Harvey Estuary, and south Harvey Estuary
 345 (see Figure 1 for their domain definition) in simulated years and future scenarios. The data were categorized into four seasons:
 346 spring (September, October, November), summer (December, January, February), autumn (March, April, May), and winter
 347 (June, July, August).

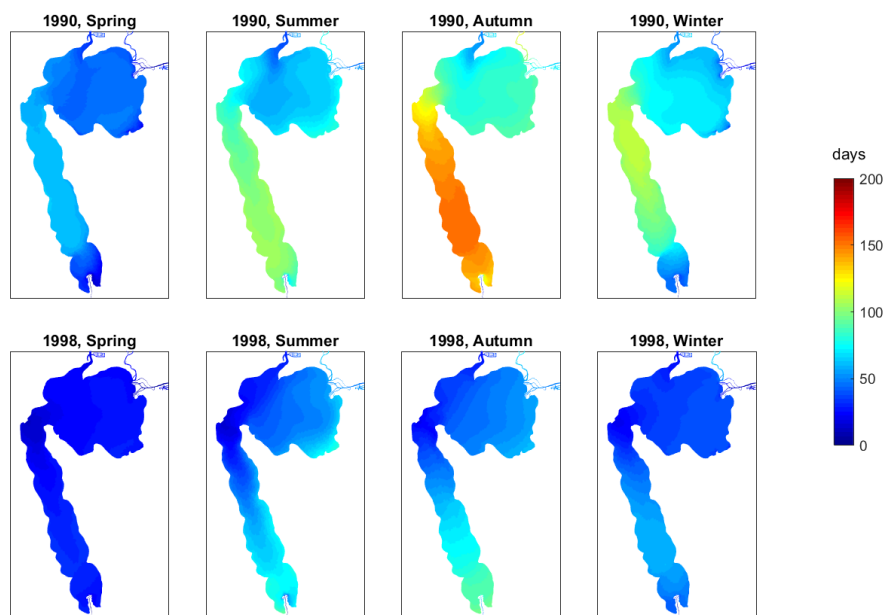
348
 349 The bulk flushing time τ_f also showed significant reduction in summer and winter due to the Cut-opening (Figure 7). The
 350 values of τ_f were much smaller than the average modelled water age in the wintertime, about 50% lower in the Cut-closed
 351 scenarios and 34%-58% lower in the Cut-open scenarios. This was not surprising as the bulk flushing time method assumes
 352 the water body is fully-mixed and corresponds to the time for the seawater and freshwater inflows to replace the lagoon water,
 353 whereas the water age method considered the heterogeneity in the spatial distribution of water retention and mixing. The spatial
 354 difference in water retention is further illustrated in Figure 8, which shows a plan-view of the seasonally-averaged water ages.
 355 The water age in the areas adjacent to the Cut entry point has been largely reduced by the Cut-opening, yet the south Harvey
 356 Lagoon and some parts of the east Peel Inlet still showed high water retention. Furthermore, the τ_f showed minor response to
 357 the drying climate after the Cut construction, indicating the exchange fraction of the seawater fluxes have been over-estimated.
 358



359

360 **Figure 7.** Comparison of average modelled water age (τ) and calculated bulk flushing time (τ_f) in (a) summertime and (b)
 361 wintertime in the PHE. The shaded areas indicate the 10% and 90% percentiles of modelled water ages.

362



363

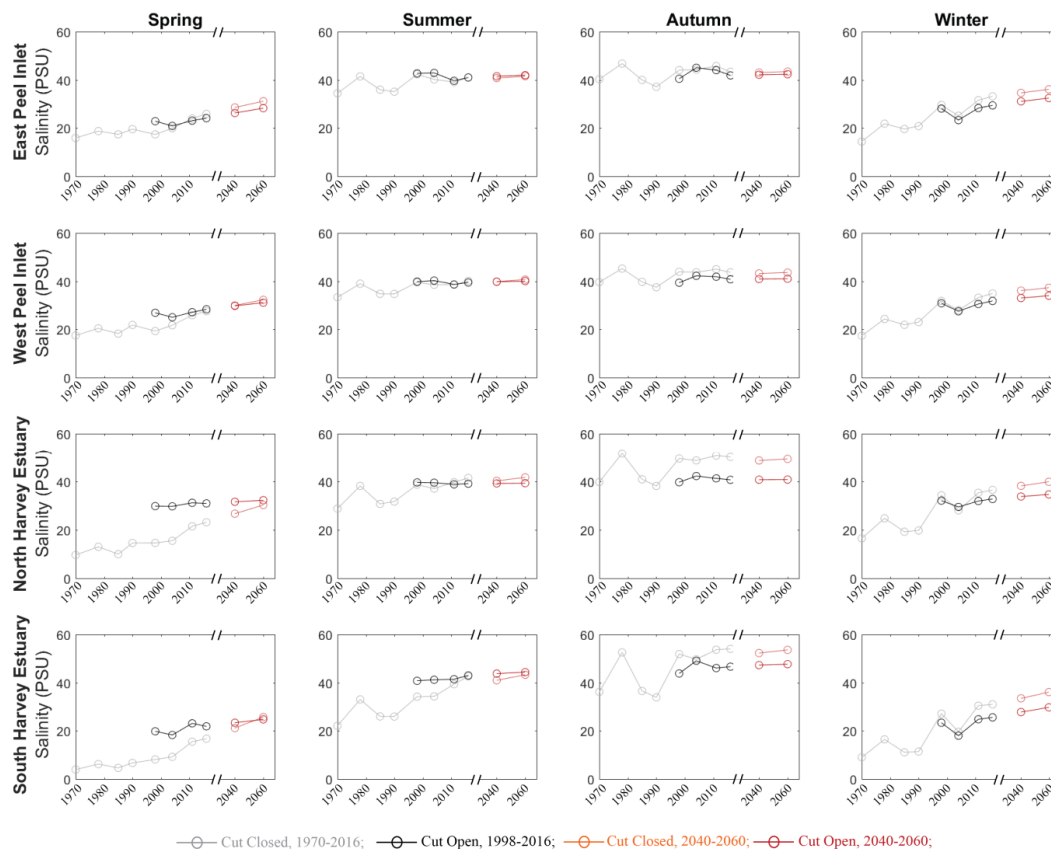
364 **Figure 8.** Spatial distribution of season-averaged water age in 1990 (top panels) and 1998 (bottom panels).

365



366 3.4 Responses of salinity and stratification to climate change and the Cut-opening

367 Similar to τ , the changes in salinity in response to the drying climate showed large variability in space and time, and the impact
 368 of the Cut-opening acted to increase salinity in the wet season, but reduced hypersalinity risks (>40 PSU) in the dry season
 369 (Figure 9). In the “no-Cut” scenarios, the mean salinity during the wet season increased from <20 PSU in 1970 to over 30 PSU
 370 in 2016. During the dry season, the changes in salinity were relatively smaller over time. The Cut-opening could increase or
 371 decrease the salinity in the estuary, depending on the salinity within the estuary at the time, compared to the ocean salinity of
 372 approximately 36 PSU. If the estuary salinity was lower than the ocean salinity, the Cut-opening tended to increase the salinity
 373 level, and vice versa. For example, the salinity in the north Harvey Estuary increased from 17.5 PSU to 28.3 PSU in the spring
 374 of 1998 by the Cut-opening, yet reduced from 51.8 to 39.8 PSU by the opening of the Cut in the autumn. The Cut-opening has
 375 a relatively smaller influence on the salinity of Peel Inlet, which is connected with the ocean via not only the Cut but also the
 376 Mandurah Channel. The projected climate is expected to slightly increase the salinity in the Peel Inlet and Harvey Estuary,
 377 mostly in the winter and spring periods.
 378



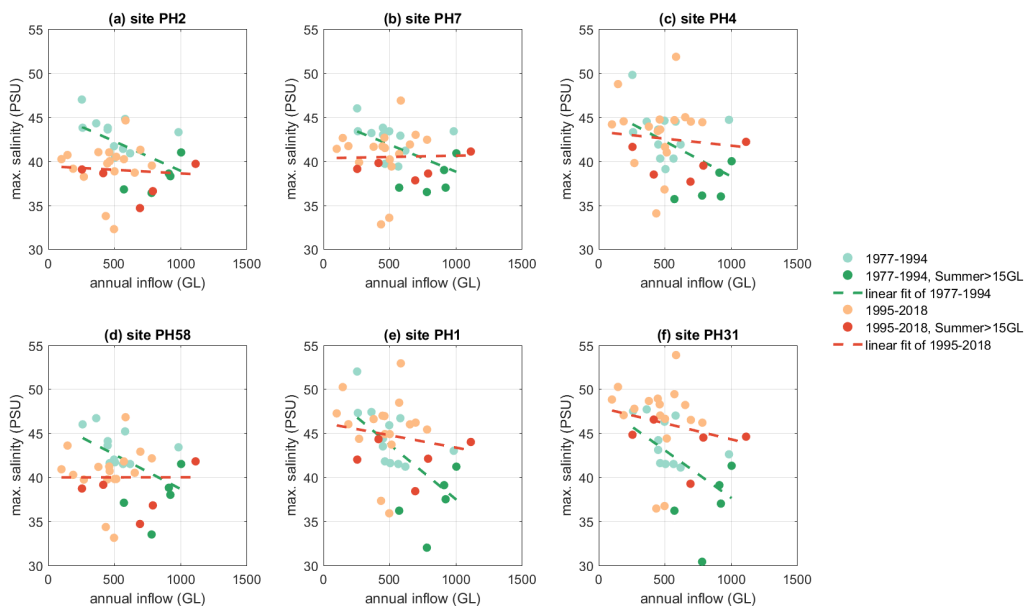
380 **Figure 9.** Changes of mean salinity in PHE in simulated years and future scenarios. Same as Figure 6 the changes are
 381 categorized into four zones and four seasons.

382



383

384 Hypersalinity was often observed in the summer and autumn seasons in the Peel Inlet from both the ‘with-Cut’ and ‘no-Cut’
385 scenarios. The Harvey Estuary shows an increasing salinity with the drying climate in summer and becomes hypersaline after
386 2011. High salinity with values over 50 PSU was observed in autumn in South Harvey Estuary in the ‘no-Cut’ scenarios, whilst
387 the Cut-opening reduced the hypersalinity risks in autumn in the Harvey Estuary. The relationships of the hypersalinity and
388 the catchment inflows are further investigated with monitoring data at six regular monitoring sites (Figure 10), which highlights
389 the maximum salinity recorded in autumn has increased with reduced inflows, especially in the period before the Cut-opening.
390 Opening of the Cut reduced the maximum salinity at the sites near the Cut (site PH2 and PH58) under an annual flow threshold
391 of about 1000 GL/year. The hypersalinity risk increases with distance from the channels, especially in site PH31 in the south
392 Harvey Estuary where salinity >45 PSU was often observed after the Cut-opening. The maximum salinity can also be affected
393 by other factors, such as unseasonal rainfall events in summer, which brought down the maximum salinity measured in March
394 (Figure 10). However, it can be concluded that the hypersalinity risks have increased in response to the catchment drying trend,
395 and the Cut-opening has reduced the sensitivity of maximum salinity to the changes in inflow rates.
396



397

398 **Figure 10.** Maximum salinity recorded in March/April and the annual inflow in the hydrologic year (March to March) at 6
399 monitoring sites (see the site locations in Figure 1). The darker symbols indicate the years with accidental summer rainfall
400 events and caused the catchment inflows higher than 15 GL.

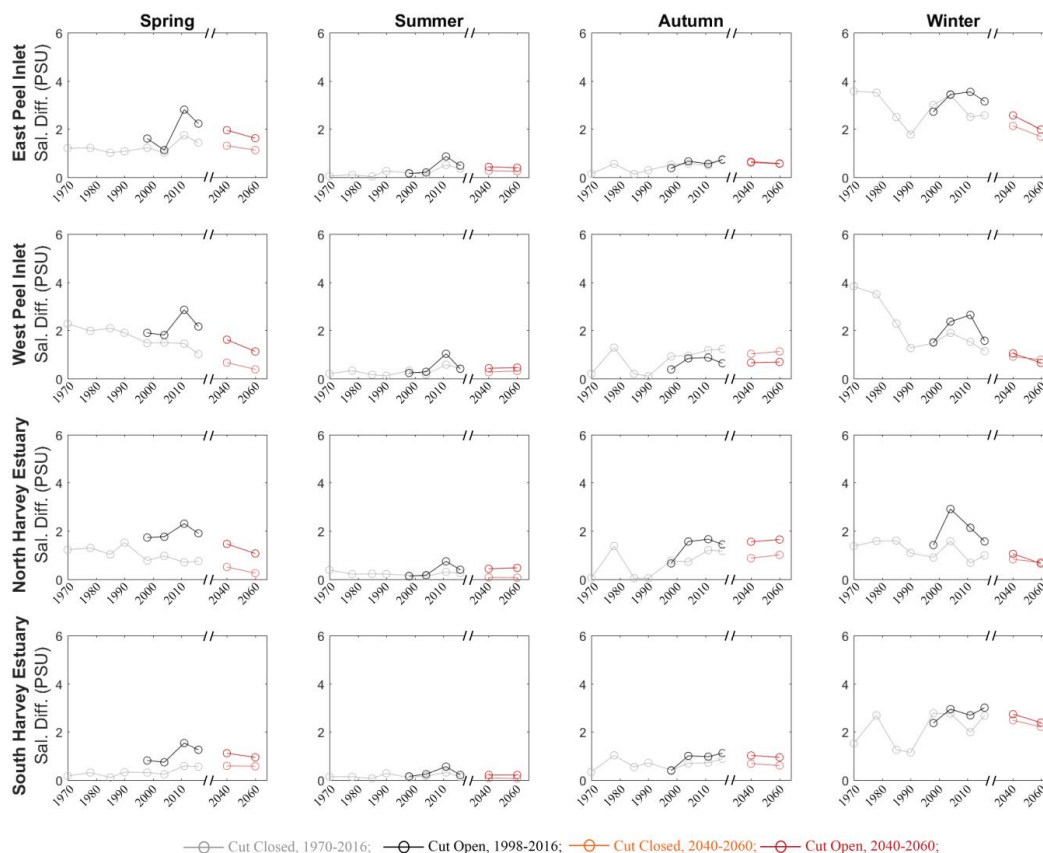
401

402

403 The magnitude of salinity stratification (salinity difference between the bottom and surface water) in winter and spring has
404 shown a declining trend with the drying climate, while the variations were small in summer and autumn (Figure 11). The
405 opening of the Cut has enhanced the rate of ocean water intrusion, which creates stronger salt-stratification during the wet



406 season when it interacts with the freshwater inflows. The salt stratification was reduced to mostly < 2 PSU in the 2060
 407 projection scenario, indicating a weaker salt-stratification due to the reduced freshwater inflows and sea level rise.
 408



410 **Figure 11.** Changes of mean salinity difference between surface and bottom waters in PHE in the simulated years and future
 411 scenarios. Same as Figure 6 the changes are categorized into four zones and four seasons.

412

413 4 Discussion

414 4.1 PHE hydrological dynamics in time and space

415 We have shown the changes in the water retention and salinity within the morphologically complex PHE system, in response
 416 to long-term changes in the relative mixture of water resources from the ocean, catchment and rainfall. The signals of climate
 417 change and human interventions in these changes, have been analysed by comparing results from the modelling scenarios to
 418 attribute each of their relative impacts separately. With the assistance of a 3D hydrodynamic model, we firstly identified the
 419 major drivers of PHE hydrology as the gradual but persistent drying trend, and the acute changes caused by the opening of the
 420 artificial channel and associated coastal engineering activities. Scenarios of declining precipitation and catchment runoff with
 421 and without the artificial channel were also explored to compare their impacts.



422

423 The results clearly showed the hydrology in PHE was profoundly changed corresponding to the reduced precipitation and
424 catchment inflow as well as to the opening of the artificial channel, although other factors such as changes in air temperature,
425 sea level rise, and benthic vegetation also affected the hydrology in much smaller scales. The results have highlighted
426 magnitudes of hydrologic changes introduced by the drying climate, and the complexity of the interacting impacts from climate
427 and the artificial channel in time and space. Firstly, the artificial channel successfully improved the estuary flushing by
428 reducing average water age by 20-110 days; while in contrast the reduced precipitation and inflow had a gradual opposite
429 effect on the water age, and during the wet season this has almost counteracted the reduction brought about by the channel.
430 Secondly, the drying climate caused an increase in the salinity by 10-30 PSU; whilst the artificial channel increased the salinity
431 during the wet season, it has reduced the likelihood of hypersalinity (>40 PSU) during the dry season in some areas.

432

433 The climate factor had not been considered in previous reports evaluating or predicting the consequence of the Cut-opening
434 when it was originally designed (Lord, 1998; Manda et al., 2014; Prestrelo and Monteiro-Neto, 2016), as the focus was on the
435 flushing benefit to reduce the accumulation of nutrients and algal biomass. The findings from this study suggest that climate
436 change has been taking effect over the period when the Cut was implemented, and from the view point of particular metrics,
437 it is now over-taking the effect of the Cut. The lessons from this case-study highlight the need to look more broadly at
438 environmental impacts when designing or operating large-scale engineering projects on coastal lagoons, due to the potential
439 for long-term non-stationarity in contributing river flows.

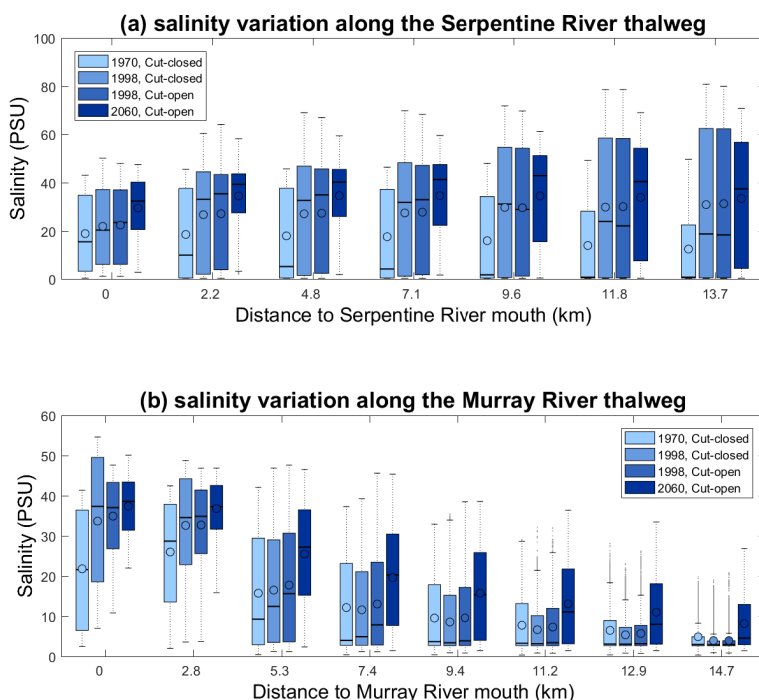
440

441 Of relevance to management, the impacts also varied spatially in this large lagoon. The water age and salinity have showed
442 distinct responses to the climate change and Cut-opening with various connection with the rivers and ocean (Figure 6 and 9).
443 The southern estuary, which has the least connection with the ocean through the natural channel, is the most sensitive to climate
444 change and the opening of the artificial channel. The bulk flushing time also showed significant reduction corresponding to
445 the Cut-opening, however, it was less sensitive to the drying climate. The results of water age distribution indicated that
446 incomplete mixing had led to area-specific retention of water, which has been labelled previously as the 'sticky water' effect
447 (Andutta et al., 2012); in this case the concept of bulk flushing time therefore needs to be used with caution in such a large
448 choked-type lagoon, because it only gives an average estimation of water retention for the whole estuary and fails to consider
449 the strong gradients in lagoon hydrodynamics. Understanding these patterns can be important to help understand local effects
450 on lagoon ecology (e.g. crab larval recruitment) and processes related to nutrient deposition and retention within the sediment.

451

452 Aside from changes in flushing and the mean salinity fields within the lagoon, the changes in the climate and ocean flushing
453 also altered the hydrology in the tidal reaches of the rivers connecting to the PHE. The annual variability of salinity along the
454 rivers (Figure 12) indicated there is an increasing risk of hypersalinity in the Serpentine River (connecting to the PHE from
455 the north) and an upward movement of the salt-wedge in the Murray River (the major inflow connecting PHE from the east).
456 For example, the mean salinity at the Serpentine River mouth was about 20 PSU in 1970, then increased to 24 PSU in 1998
457 and projected to increase to over 30 PSU in 2060. In the upstream areas of the Serpentine River, the mean salinity increased
458 from about 15 PSU in 1970 to near 35 PSU in 2060. While there is less hypersalinity risk in the Murray River due to larger
459 volumes of freshwater flushing, there is also a trend of increasing salinity along the river with the drying climate. The
460 differences between the Cut-closed and Cut-open scenarios in year 1998 are much smaller than those caused by the drying
461 climate, which indicates that the drying climate is the major cause of the salinity changes in the rivers.

462



463

464 **Figure 12.** Longitudinal gradient in annual salinity variability in four selected scenarios (1970, 1998 without the Cut opening,
465 1998 with the Cut opening, and a future scenario 2060 with assumptions of reduced flow and sea level rise) moving upstream
466 along the (a) Serpentine River and (b) Murray River.

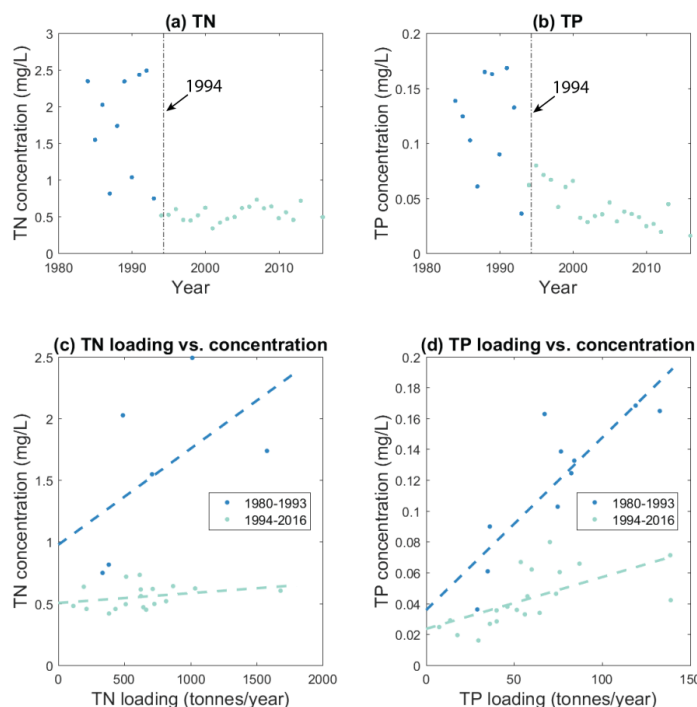
467

468

469 4.2 Applications for estuary ecosystem management

470 The Cut had an obvious and dramatic effect on increasing the export of nutrients that would have otherwise been retained
471 (Figure 13). Since the Cut opening in 1994 the main monitoring stations have shown TN as being stable around 0.5mg/L and
472 TP has declined from 0.05 to 0.02 mg/L over time. Importantly, the increasing rate of exchange has made the estuary
473 concentration of nutrients less sensitive to the inflow load (as demonstrated by the reduction in slope of 11c and 11d). The
474 results have also revealed an increase in τ associated with the drying climate that has eroded some of the benefits associated
475 with increased flushing following the construction of the Cut, and further reductions in flows will cause less flushing and will
476 likely lead to a tendency for increasing nutrient accumulation over time.

477



478

479 **Figure 13.** Changes in the mean nutrient concentration of (a) TN and (b) TP in the Peel-Harvey Estuary (based on the average
480 of the 6 main monitoring stations), and their relationship with the total annual nutrient loading (c and d).

481

482

483 The hydrologic changes led not only to changes in the nutrient concentrations but also the mean salinity, with potential
484 ramifications for the ecological community. In particular, the phytoplankton biomass dropped dramatically since the Cut
485 opening (Figure 2) due to the improvement of ocean connectivity and flushing, but also due to a less desirable salinity regime
486 in summertime for the toxic cyanobacteria *Nodularia spumigena* that plagued the Harvey Estuary before the Cut opening.
487 Field observations also showed that the biomass of macroalgae has decreased in the Peel Inlet, while it has increased in the
488 Harvey Estuary since the Cut opening, which potentially reflects the reduced nutrient concentrations, increased salinity and
489 greater light availability (Pedretti et al., 2011). The biomass of some benthic macroinvertebrates, such as the blue swimmer
490 crabs (*Portunus armatus*) and the Western king prawn (*Penaeus latisulcatus*) also showed an increase with the Cut opening
491 and the reduced flow in recent years (Bradby, 1997; Johnston et al., 2014). The changes in the biological communities
492 corresponding to the hydrologic changes seem to remain in the predicted future as the projected drying climate led to constant
493 low flushing and high salinity in this estuary.

494

495 **4.3 Uncertainty of future hydrology**

496 This study has investigated the hydrologic changes in selected historical years and under projected future drying climate.
497 However, the drying climate was predicted with a combination of climate models (Smith and Power, 2014) and the annual
498 perturbations in future climate and their impacts on the hydrology remain the subject of uncertainty. As shown in Cloern et al.
499 (2016), the hydrology of lagoons has been changing at a faster pace in the past decade from a combination of human activity



500 and climate variability. The sea level of the ocean adjacent to the PHE has been rising at faster speeds in the past decades
501 (Kuhn et al., 2011). The PHE catchment is also undergoing fast development due to the increasing population and agricultural
502 expansion (Kelsey et al., 2011). Intensification of human activities, such as water consumption and diversion, will further
503 affect the lagoon's hydrology and associated ecosystem, but how these factors will change in future remains unclear. Therefore,
504 our results related to the future prediction are simply to indicate the possible changes of hydrology under the projected drying
505 climate in order to highlight the general trend and allow for prioritisation of adaptation strategies such as environmental water
506 allocation policies. Continuous monitoring on the hydrology and water quality of the lagoon and its catchment must therefore
507 be prioritised to closely observe further hydrologic change in order to provide prompt actions for management.

508 **5 Conclusions and outlook**

509 This study has sought to analyse the hydrologic changes in the Peel-Harvey Estuary to a range of drivers, and focused on the
510 effects of the recent climate change trend on the hydrologic evolution in the Peel-Harvey Estuary, relative to the changes
511 brought about by construction of the Dawesville Cut. Our results suggested the climate change in the past decades has a
512 remarkable effect on the hydrology with the same magnitude as that caused by the opening of an artificial channel, and also
513 highlighted the complexity of their interactions. The artificial channel was effective in reducing the water retention time
514 especially in areas close to the channel, while the drying climate trend has acted to increase the water retention time. The
515 artificial channel enhanced the ocean intrusion, which had a mutual effect with the drying climate to increase the estuary
516 salinity during the wet season, but it had opposite effect of reducing the hypersalinity during the dry season. The artificial
517 channel increased the seawater fluxes and the salinity stratification, mostly in the Harvey Estuary, while the drying climate
518 reduced the salinity stratification in the main body of the estuary. The changes in nutrient levels and habitat of pelagic and
519 benthic communities related to hydrology are also discussed, which showed the communities are sensitive to the hydrologic
520 changes. Consideration of the projected drying trend is essential in designing management plans associated with planning for
521 environmental water provision and setting water quality loading targets.

522

523



524 **Data availability**

525 The datasets generated during the current study are available from the corresponding author on request.

526 **Author contribution**

527 All the authors contributed to the design of the study. Peisheng Huang carried the hydrology modelling work and prepared the
528 first draft of the manuscript. Karl Henig provided the catchment outputs of the inflow rates and nutrient concentrations. Jatin
529 Kala and Julia Andrys provided the WRF weather data. Matthew R. Hipsey was the project leader and provided technical and
530 financial supports. Jatin Kala and Matthew R. Hipsey helped to interpret the model data and write the article.
531

532 **Competing interests**

533 The authors declare no competing financial or non-financial interest.

534

535



536 **References**

- 537 Almroth-Rosell, E., Edman, M., Eilola, K., Markus Meier, H. E. and Sahlberg, J.: Modelling nutrient retention in the coastal
538 zone of an eutrophic sea, *Biogeosciences*, 13(20), 5753–5769, doi:10.5194/bg-13-5753-2016, 2016.
- 539 Andrys, J., Lyons, T. J. and Kala, J.: Multidecadal evaluation of WRF downscaling capabilities over Western Australia in
540 simulating rainfall and temperature extremes, *J. Appl. Meteorol. Climatol.*, 54(2), 370–394, doi:10.1175/JAMC-D-14-0212.1,
541 2015.
- 542 Andrys, J., Lyons, T. J. and Kala, J.: Evaluation of a WRF ensemble using GCM boundary conditions to quantify mean and
543 extreme climate for the southwest of Western Australia (1970–1999), *Int. J. Climatol.*, 36(13), 4406–4424,
544 doi:10.1002/joc.4641, 2016.
- 545 Andrys, J., Kala, J. and Lyons, T. J.: Regional climate projections of mean and extreme climate for the southwest of Western
546 Australia (1970–1999 compared to 2030–2059), *Clim. Dyn.*, 48(5–6), 1723–1747, doi:10.1007/s00382-016-3169-5, 2017.
- 547 Andutta, F. P., Kingsford, M. J. and Wolanski, E.: 'Sticky water' enables the retention of larvae in a reef mosaic, *Estuar. Coast.*
548 *Shelf Sci.*, 101, 54–63, doi:10.1016/j.ecss.2012.02.013, 2012.
- 549 Basset, A., Elliott, M., West, R. J. and Wilson, J. G.: Estuarine and lagoon biodiversity and their natural goods and services,
550 *Estuar. Coast. Shelf Sci.*, 132, 1–4, doi:10.1016/j.ecss.2013.05.018, 2013.
- 551 Bates, B. C., Hope, P., Ryan, B., Smith, I. and Charles, S.: Key findings from the Indian Ocean Climate Initiative and their
552 impact on policy development in Australia, *Clim. Change*, 89(3–4), 339–354, doi:10.1007/s10584-007-9390-9, 2008.
- 553 Bicknell, C.: Review of Sand Bypassing Dawesville and Mandurah: Coastal Engineering Investigation, Department for
554 Planning and Infrastructure. [online] Available from: <https://books.google.com.au/books?id=CA46NAAACAAJ>, 2006.
- 555 Black, R. E. and Rosher, J.: The Peel Inlet and Harvey Estuary System hydrology and meteorology. Part of the Peel Inlet and
556 Harvey Estuary Environmental Study, Dept. of Conservation and Environment., 1980.
- 557 BMT WBM: TUFLOW FV Science Manual, , 1–29, 2013.
- 558 Brearley, A.: Ernest Hodgkin's Swanland: the estuaries and coastal lagoons of south-western Australia, UWA Publishing.,
559 2005.
- 560 Bruce, L. C., Cook, P. L. M., Teakle, I. and Hipsey, M. R.: Hydrodynamic controls on oxygen dynamics in a riverine salt
561 wedge estuary, the Yarra River estuary, Australia, *Hydrol. Earth Syst. Sci.*, 18(4), 1397–1411, doi:10.5194/hess-18-1397-
562 2014, 2014.
- 563 Cloern, J. E., Abreu, P. C., Carstensen, J., Chauvaud, L., Elmgren, R., Grall, J., Greening, H., Johansson, J. O. R., Kahru, M.,
564 Sherwood, E. T., Xu, J. and Yin, K.: Human activities and climate variability drive fast-paced change across the world's
565 estuarine-coastal ecosystems, *Glob. Chang. Biol.*, 22(2), 513–529, doi:10.1111/gcb.13059, 2016.
- 566 Cloern, J. E., Jassby, A. D., Schraga, T. S., Nejad, E. and Martin, C.: Ecosystem variability along the estuarine salinity gradient:
567 Examples from long-term study of San Francisco Bay, *Limnol. Oceanogr.*, 62, S272–S291, doi:10.1002/lno.10537, 2017.
- 568 Cottingham, A., Hesp, S. A., Hall, N. G., Hipsey, M. R. and Potter, I. C.: Marked deleterious changes in the condition, growth
569 and maturity schedules of *Acanthopagrus butcheri* (Sparidae) in an estuary reflect environmental degradation, *Estuar. Coast.*
570 *Shelf Sci.*, 149, 109–119, doi:10.1016/j.ecss.2014.07.021, 2014.
- 571 Ducharme, A., Baubion, C., Beaudoin, N., Benoit, M., Billen, G., Brisson, N., Garnier, J., Kieken, H., Lebonvallet, S., Ledoux,
572 E., Mary, B., Mignolet, C., Poux, X., Sauboua, E., Schott, C., Théry, S. and Viennot, P.: Long term prospective of the Seine
573 River system: Confronting climatic and direct anthropogenic changes, *Sci. Total Environ.*, 375(1–3), 292–311,
574 doi:10.1016/j.scitotenv.2006.12.011, 2007.
- 575 Dufour, P., Andréfouët, S., Charpy, L. and Garcia, N.: Atoll morphometry controls lagoon nutrient regime, *Limnol. Oceanogr.*,
576 46(2), 456–461, doi:10.4319/lo.2001.46.2.0456, 2001.
- 577 Environmental Protection Authority, W. A.: Water Quality Improvement Plan for the Rivers and Estuary of the Peel-Harvey
578 System - Phosphorus Management. [online] Available from: <http://internal-pdf/Water Quality Improvement Plan for the Rivers and Estuary of -1288010496/Water Quality Improvement Plan for the Rivers and Estuary of the Peel-Harvey System - Phosphorus Management.pdf>, 2008.
- 581 Ferrarin, C., Ghezzi, M., Umgiesser, G., Tagliapietra, D., Camatti, E., Zaggia, L. and Sarretta, A.: Assessing hydrological
582 effects of human interventions on coastal systems: Numerical applications to the Venice Lagoon, *Hydrol. Earth Syst. Sci.*,
583 17(5), 1733–1748, doi:10.5194/hess-17-1733-2013, 2013.
- 584 Ferreira, J. G., Wolff, W. J., Simas, T. C. and Bricker, S. B.: Does biodiversity of estuarine phytoplankton depend on



- 585 hydrology?, *Ecol. Modell.*, 187(4), 513–523, doi:10.1016/j.ecolmodel.2005.03.013, 2005.
- 586 Feyrer, F., Cloern, J. E., Brown, L. R., Fish, M. A., Hieb, K. A. and Baxter, R. D.: Estuarine fish communities respond to
587 climate variability over both river and ocean basins, *Glob. Chang. Biol.*, 21(10), 3608–3619, doi:10.1111/gcb.12969, 2015.
- 588 Finlayson, B. L. and McMahon, T. A.: Australia v the world: a comparative analysis of streamflow characteristics, *Fluv.*
589 *Geomorphol. Aust.*, 17–40, 1988.
- 590 Firth, R., Kala, J., Lyons, T. J. and Andrys, J.: An analysis of regional climate simulations for Western Australia’s wine
591 regions-model evaluation and future climate projections, *J. Appl. Meteorol. Climatol.*, 56(7), 2113–2138, doi:10.1175/JAMC-
592 D-16-0333.1, 2017.
- 593 Fischer, H. B., List, E. J., Koh, R. C. Y., Imberger, J. and Brooks, N. H.: Chapter 7 - Mixing in Estuaries, edited by H. B.
594 FISCHER, E. J. LIST, R. C. Y. KOH, J. IMBERGER, and N. H. B. T.-M. in I. and C. W. BROOKS, pp. 229–278, Academic
595 Press, San Diego., 1979.
- 596 Fofonoff, N. P. and Millard, R. C.: Algorithms for computation of fundamental properties of seawater, UNESCO Tech. Pap.
597 *Mar. Sci.*, 44, 53, doi:10.1111/j.1365-2486.2005.001000.x, 1983.
- 598 Gentili, J.: *Climates of Australia and New Zealand*, Elsevier., 1971.
- 599 Ghezzi, M., Guerzoni, S., Cucco, A. and Umgiesser, G.: Changes in Venice Lagoon dynamics due to construction of mobile
600 barriers, *Coast. Eng.*, 57(7), 694–708, doi:10.1016/j.coastaleng.2010.02.009, 2010.
- 601 Gillanders, B. M., Elsdon, T. S., Halliday, I. A., Jenkins, G. P., Robins, J. B. and Valesini, F. J.: Potential effects of climate
602 change on Australian estuaries and fish utilising estuaries: A review, *Mar. Freshw. Res.*, 62(9), 1115–1131,
603 doi:10.1071/MF11047, 2011.
- 604 Gong, W., Shen, J. and Jia, J.: The impact of human activities on the flushing properties of a semi-enclosed lagoon: Xiaohai,
605 Hainan, China, *Mar. Environ. Res.*, 65(1), 62–76, doi:10.1016/j.marenvres.2007.08.001, 2008.
- 606 Hallett, C. S., Hobday, A. J., Tweedley, J. R., Thompson, P. A., McMahon, K. and Valesini, F. J.: Observed and predicted
607 impacts of climate change on the estuaries of south-western Australia, a Mediterranean climate region, *Reg. Environ. Chang.*,
608 18(5), 1357–1373, doi:10.1007/s10113-017-1264-8, 2018.
- 609 Hirsch, A. L., Evans, J. P., Di Virgilio, G., Perkins-Kirkpatrick, S. E., Argüeso, D., Pitman, A. J., Carouge, C. C., Kala, J.,
610 Andrys, J., Petrelli, P. and Rockel, B.: Amplification of Australian Heatwaves via Local Land-Atmosphere Coupling, *J.*
611 *Geophys. Res. Atmos.*, 124(24), 13625–13647, doi:10.1029/2019JD030665, 2019.
- 612 Howarth, R. W. and Marino, R.: Nitrogen as the limiting nutrient for eutrophication in coastal marine ecosystems: Evolving
613 views over three decades, *Limnol. Oceanogr.*, 51(1part2), 364–376, doi:10.4319/lo.2006.51.1_part_2.0364, 2006.
- 614 Huang, P., Kilminster, K., Larsen, S. and Hipsey, M. R.: Assessing artificial oxygenation in a riverine salt-wedge estuary with
615 a three-dimensional finite-volume model, *Ecol. Eng.*, 118(August 2017), 111–125, doi:10.1016/j.ecoleng.2018.04.020, 2018.
- 616 IPCC: WGI AR4 - The Physical Science Basis, *Mitig. Clim. Chang.*, 996, 1–1007,
617 doi:http://dx.doi.org/10.1017/CBO9780511546013, 2007.
- 618 Izrael, Y. A., Semenov, S. M., Anisimov, O. A., Anokhin, Y. A., Velichko, A. A., Revich, B. A. and Shiklomanov, I. A.: The
619 Fourth Assessment Report of the Intergovernmental Panel on Climate Change: Working Group II contribution, *Russ. Meteorol.*
620 *Hydrol.*, 32(9), 551–556, doi:10.3103/S1068373907090014, 2007.
- 621 Jouon, A., Douillet, P., Ouillon, S. and Fraunie, P.: Calculations of hydrodynamic time parameters in a semi-opened coastal
622 zone using a 3D hydrodynamic model, *Cont. Shelf Res.*, 26, 1395–1415, doi:10.1016/j.csr.2005.11.014, 2006.
- 623 Kala, J., Andrys, J., Lyons, T. J., Foster, I. J. and Evans, B. J.: Sensitivity of WRF to driving data and physics options on a
624 seasonal time-scale for the southwest of Western Australia, *Clim. Dyn.*, 44(3–4), 633–659, doi:10.1007/s00382-014-2160-2,
625 2015.
- 626 Kasai, A., Kurikawa, Y., Ueno, M., Robert, D. and Yamashita, Y.: Salt-wedge intrusion of seawater and its implication for
627 phytoplankton dynamics in the Yura Estuary, Japan, *Estuar. Coast. Shelf Sci.*, 86(3), 408–414, doi:10.1016/j.ecss.2009.06.001,
628 2010.
- 629 Kelsey, P., Hall, J., Kretschmer, P., Quilton, B. and Shakya, D.: Hydrological and nutrient modelling of the Peel-Harvey
630 catchment, *Water Science Technical Series*, Report no. 33, Department of Water, Western Australia., 2011.
- 631 Kjerfve, B., Schettini, C. A. F., Knoppers, B., Lessa, G. and Ferreira, H. O.: Hydrology and salt balance in a large, hypersaline
632 coastal lagoon: Lagoa de Araruama, Brazil, *Estuar. Coast. Shelf Sci.*, 42(6), 701–725, doi:10.1006/ecss.1996.0045, 1996.



- 633 Knoppers, B., Kjerfve, B. and Carmouze, J. P.: Trophic state and water turn-over time in six choked coastal lagoons in Brazil,
634 *Biogeochemistry*, 14(2), 149–166, doi:10.1007/BF00002903, 1991.
- 635 Kuhn, M., Tuladhar, D. and Corner, R.: Visualising the spatial extent of predicted coastal zone inundation due to sea level rise
636 in south-west Western Australia, *Ocean Coast. Manag.*, 54(11), 796–806, doi:10.1016/j.ocecoaman.2011.08.005, 2011.
- 637 Legović, T., Žutić, V., Gržetić, Z., Cauwet, G., Precali, R. and Viličić, D.: Eutrophication in the Krka estuary, *Mar. Chem.*,
638 46(1–2), 203–215, doi:10.1016/0304-4203(94)90056-6, 1994.
- 639 Liu, W.-C. and Chan, W.-T.: Assessment of Climate Change Impacts on Water Quality in a Tidal Estuarine System Using a
640 Three-Dimensional Model, *Water*, 8(2), 60, doi:10.3390/w8020060, 2016.
- 641 Lloret, J., Marín, A. and Marín-Guirao, L.: Is coastal lagoon eutrophication likely to be aggravated by global climate change?,
642 *Estuar. Coast. Shelf Sci.*, 78(2), 403–412, doi:10.1016/j.ecss.2008.01.003, 2008.
- 643 Lord, D. A.: Dawesville Channel Monitoring Programme , Water and Rivers Commission., 1998.
- 644 Manda, A. K., Giuliano, A. S. and Allen, T. R.: Influence of artificial channels on the source and extent of saline water intrusion
645 in the wind tide dominated wetlands of the southern Albemarle estuarine system (USA), *Environ. Earth Sci.*, 71(10), 4409–
646 4419, doi:10.1007/s12665-013-2834-9, 2014.
- 647 Monsen, N. E., Cloern, J. E., Lucas, L. V. and Monismith, S. G.: A comment on the use of flushing time, residence time, and
648 age as transport time scales, *Limnol. Oceanogr.*, 47(5), 1545–1553, doi:10.4319/lo.2002.47.5.1545, 2002.
- 649 Newton, A., Icely, J., Cristina, S., Brito, A., Cardoso, A. C., Colijn, F., Riva, S. D., Gertz, F., Hansen, J. W., Holmer, M.,
650 Ivanova, K., Leppäkoski, E., Canu, D. M., Mocenni, C., Mudge, S., Murray, N., Pejrup, M., Razinkovas, A., Reizopoulou, S.,
651 Pérez-Ruzafa, A., Schernewski, G., Schubert, H., Carr, L., Solidoro, C., Viaroli, P. and Zaldívar, J. M.: An overview of
652 ecological status, vulnerability and future perspectives of European large shallow, semi-enclosed coastal systems, lagoons and
653 transitional waters, *Estuar. Coast. Shelf Sci.*, 140, 95–122, doi:10.1016/j.ecss.2013.05.023, 2014.
- 654 Newton, A., Brito, A. C., Icely, J. D., Derolez, V., Clara, I., Angus, S., Schernewski, G., Inácio, M., Lillebø, A. I., Sousa, A.
655 I., Béjaoui, B., Solidoro, C., Tosic, M., Cañedo-Argüelles, M., Yamamuro, M., Reizopoulou, S., Tseng, H. C., Canu, D.,
656 Roselli, L., Maanan, M., Cristina, S., Ruiz-Fernández, A. C., Lima, R. F. d., Kjerfve, B., Rubio-Cisneros, N., Pérez-Ruzafa,
657 A., Marcos, C., Pastres, R., Pranovi, F., Snoussi, M., Turpie, J., Tuchkovenko, Y., Dyack, B., Brookes, J., Povilanskas, R. and
658 Khokhlov, V.: Assessing, quantifying and valuing the ecosystem services of coastal lagoons, *J. Nat. Conserv.*, 44(February),
659 50–65, doi:10.1016/j.jnc.2018.02.009, 2018.
- 660 Odebrecht, C., Abreu, P. C. and Carstensen, J.: Retention time generates short-term phytoplankton blooms in a shallow
661 microtidal subtropical estuary, *Estuar. Coast. Shelf Sci.*, 162, 35–44, doi:10.1016/j.ecss.2015.03.004, 2015.
- 662 Paerl, H. W., Valdes, L. M., Peierls, B. L., Adolf, J. E. and Harding, L. W.: Anthropogenic and climatic influences on the
663 eutrophication of large estuarine ecosystems, *Limnol. Oceanogr.*, 51(1_part_2), 448–462,
664 doi:10.4319/lo.2006.51.1_part_2.0448, 2006.
- 665 Paerl, H. W., Hall, N. S., Peierls, B. L., Rossignol, K. L. and Joyner, A. R.: Hydrologic Variability and Its Control of
666 Phytoplankton Community Structure and Function in Two Shallow, Coastal, Lagoonal Ecosystems: The Neuse and New River
667 Estuaries, North Carolina, USA, *Estuaries and Coasts*, 37(S1), 31–45, doi:10.1007/s12237-013-9686-0, 2014.
- 668 Pedretti, Y. M., Kobryn, H. T., Sommerville, E. F. and Wienczugow, K.: Snapshot Survey of the Distribution and Abundance
669 of Seagrass and Macroalgae in the Peel-Harvey Estuary from November / December 2009 Report to Department of Water,
670 Rep. to Dep. Water by Mar. Freshw. Res. Lab. Rep. number MAFRL, 11(February), 2011.
- 671 Pérez-Ruzafa, A., Marcos, C. and Pérez-Ruzafa, I. M.: Mediterranean coastal lagoons in an ecosystem and aquatic resources
672 management context, *Phys. Chem. Earth*, 36(5–6), 160–166, doi:10.1016/j.pce.2010.04.013, 2011.
- 673 Petersen, J. K., Hansen Würigler, J., Laursen Brogaard, M., Clausen, P., Carstensen, J. and Conley, D. J.: Regime shift in a
674 coastal marine ecosystem, *Ecol. Appl.*, 18(2), 497–510, doi:10.1890/07-0752.1, 2008.
- 675 Potter, I. C., Chuwen, B. M., Hoeksema, S. D. and Elliott, M.: The concept of an estuary: A definition that incorporates systems
676 which can become closed to the ocean and hypersaline, *Estuar. Coast. Shelf Sci.*, 87(3), 497–500,
677 doi:10.1016/j.ecss.2010.01.021, 2010.
- 678 Prestrelo, L. and Monteiro-Neto, C.: Before-after environmental impact assessment of an artificial channel opening on a south-
679 western Atlantic choked lagoon system, *J. Fish Biol.*, 89(1), 735–752, doi:10.1111/jfb.13012, 2016.
- 680 Rogers, P., Hall, N. and Valesini, F.: Science Strategy for the Peel- Harvey Estuary Prepared for the Peel-Harvey Catchment
681 Council. [online] Available from: http://www.peel-harvey.org.au/wp-content/uploads/2010_Science_Strategy.pdf, 2010.
- 682 Rynne, P., Reniers, A., van de Kreeke, J. and MacMahan, J.: The effect of tidal exchange on residence time in a coastal



- 683 embayment, *Estuar. Coast. Shelf Sci.*, 172, 108–120, doi:10.1016/j.ecss.2016.02.001, 2016.
- 684 Sahu, B. K., Pati, P. and Panigrahy, R. C.: Environmental conditions of Chilika Lake during pre and post hydrological
685 intervention: An overview, *J. Coast. Conserv.*, 18(3), 285–297, doi:10.1007/s11852-014-0318-z, 2014.
- 686 Sheldon, J. E. and Alber, M.: The calculation of estuarine turnover times using freshwater fraction and tidal prism models: a
687 critical evaluation, *Estuaries and Coasts*, 29(1), 133–146, 2006.
- 688 Shi, J., Li, G., Wang, P., Beach, W. P., Shit, J., Lift, G. and Wang, P.: Anthropogenic Influences on the Tidal Prism and Water
689 Exchanges in Jiaozhou Bay, Qingdao, China, *J. Coast. Res.*, 27(1), 57–72, 2019.
- 690 Silberstein, R. P., Aryal, S. K., Durrant, J., Pearcey, M., Braccia, M., Charles, S. P., Boniecka, L., Hodgson, G. A., Bari, M.
691 A., Viney, N. R. and McFarlane, D. J.: Climate change and runoff in south-western Australia, *J. Hydrol.*, 475, 441–455,
692 doi:10.1016/j.jhydrol.2012.02.009, 2012.
- 693 Smith, I. and Power, S.: Past and future changes to inflows into Perth (Western Australia) dams, *J. Hydrol. Reg. Stud.*, 2, 84–
694 96, doi:10.1016/j.ejrh.2014.08.005, 2014.
- 695 Umlauf, L., Burchard, H. and Bolding, K.: GOTM-Sourcecode and Test Case Documentation, *Softw. Man.*, 346 [online]
696 Available from: <http://www.gotm.net/pages/documentation/manual/stable/pdf/a4.pdf>, 2012.
- 697 Valesini, F. J., Hallett, C. S., Hipsey, M. R., Kilminster, K. L., Huang, P. and Hennig, K.: Peel-Harvey Estuary, Western
698 Australia, in *Coasts and Estuaries*, pp. 103–120, Elsevier., 2019.
- 699 Di Virgilio, G., Evans, J. P., Di Luca, A., Olson, R., Argüeso, D., Kala, J., Andrys, J., Hoffmann, P., Katzfey, J. J. and Rockel,
700 B.: Evaluating reanalysis-driven CORDEX regional climate models over Australia: model performance and errors, *Clim. Dyn.*,
701 53(5–6), 2985–3005, doi:10.1007/s00382-019-04672-w, 2019.
- 702 Watanabe, K., Kasai, A., Antonio, E. S., Suzuki, K., Ueno, M. and Yamashita, Y.: Influence of salt-wedge intrusion on
703 ecological processes at lower trophic levels in the Yura Estuary, Japan, *Estuar. Coast. Shelf Sci.*, 139, 67–77,
704 doi:10.1016/j.ecss.2013.12.018, 2014.
- 705 Welsh, W.D., Vaze, J., Dutta, D., Rassam, D., Rahman, J.M., Jolly, I.D., Wallbrink, P., Podger, G.M., Bethune, M., Hardy,
706 M.J., Teng, J. and Lerat, J.: An integrated modelling framework for regulated river systems, *Environ. Model. Softw.*, 39, 81–
707 102, doi:10.1016/j.envsoft.2012.02.022, 2013.
- 708 Whitehead, P. G., Wilby, R. L., Battarbee, R. W., Kernan, M. and Wade, A. J.: A review of the potential impacts of climate
709 change on surface water quality, *Hydrol. Sci. J.*, 54(1), 101–121, doi:10.1623/hysj.54.1.101, 2009.
- 710 Williamson, S. C., Rheuban, J. E., Costa, J. E., Glover, D. M. and Doney, S. C.: Assessing the Impact of Local and Regional
711 Influences on Nitrogen Loads to Buzzards Bay, MA, *Front. Mar. Sci.*, 3(January), 279, doi:10.3389/fmars.2016.00279, 2017.
- 712 Zaldívar, J., Cardoso, A. C., Viaroli, P., Wit, R. De, Ibañez, C., Reizopoulou, S., Razinkovas, A., Basset, A., Holmer, M. and
713 Murray, N.: Eutrophication in transitional waters: an overview, *TWM, Transit. Waters Monogr.*, 1(2008), 1–78,
714 doi:10.1285/i18252273v2n1p1, 2008.
- 715 Zhu, Y., McCowan, A. and Cook, P. L. M.: Effects of changes in nutrient loading and composition on hypoxia dynamics and
716 internal nutrient cycling of a stratified coastal lagoon, *Biogeosciences*, 14(19), 4423–4433, doi:10.5194/bg-14-4423-2017,
717 2017.
- 718